Journal Name

ARTICLE

Synthesis and characterization of DNA-quantum dot conjugates for the fluorescent ratiometric detection of unlabelled DNA

L. E. Page, X. Zhang, C. M. Tyrakowski, C.-T. Ho and P. T. Snee*

Received 00th January 20xx,
Accepted 00th January 20xx

DOI: 10.1039/x0xx00000x

www.rsc.org/

A quantum dot-based ratiometrically responsive fluorescent sensor for unlabeled single-stranded DNA (ssDNA) is reported. Several technical issues concerning the development of high yield ssDNA-QD conjugation chemistry were addressed. The DNA sensor was synthesized by conjugating methacrylic phosphoramidite-functional oligonucleotides to water-soluble cadmium zinc sulfide core / zinc sulfide shell quantum dots (CdZnS/ZnS QDs). Duplex DNA was formed when the QD-bound ssDNA was incubated with its compliment. Next, titration with PicoGreen resulted in FRET energy is transfer from the dot to the dsDNA intercalating dye. The resulting ratio of the dye to QD integrated emissions is a calibratable metric for label-free DNA detection with a LOD of 3.8 nmol.

Introduction

The quantitative and selective detection of DNA significantly aids basic research on genetic diseases, medical diagnoses, and treatments. Cancer,[1] human immunodeficiency virus,[2] cholera,[3] and Lyme's disease[4] can be diagnosed via DNA identification. As such, creating biological sensors and probes for DNA is topical, and in the past decade the use of quantum dots in this regard has become of significant interest. Quantum dots (QDs, or nanocrystals) form an ideal base for creating fluorescent sensing systems due to their electrochemical and photophysical properties.[5] QDs are superior to organic fluorophores as biomarkers due to their high fluorescence efficiencies, long lifetimes, and resistance to photobleaching.[6, 7] However, their usage also has major drawbacks due to the known difficulties with water-solubilization and functionalization to impart sensitivity to chemical and/or biological analytes.[8]

Several methods have been developed to detect single-stranded DNA (ssDNA) using QD-based platforms. One of the most common motifs incorporates a molecular beacon approach based on fluorescent resonant energy transfer (FRET) modulation.[9] These systems are comprised of a single-strand oligonucleotide that is conjugated to a fluorescent QD at one end and an organic quencher moiety at the other.[10, 11] The sequence of the oligonucleotide is designed such that it preferentially base pairs with itself near the 3' and 5' ends to form a stem-loop structure. This brings the quencher in close contact with the quantum dot, resulting in significant fluorescence suppression due to the fact that QDs are excellent FRET donors.[12-14] The stem-loop structure opens upon analyte binding to form double-strand DNA

[a] Department of Chemistry, the University of Illinois at Chicago, 845 W. Taylor St. Chicago Il 60607-2405

Electronic Supplementary Information (ESI) available: Characterization data of CdZnS/ZnS quantum dots, schemes for the synthesis and usage of QD-ssDNA sensors, and additional data on sensor performance for analytes and control samples (both mismatch ssDNA samples and blanks). See DOI: 10.1039/x0xx00000x

(dsDNA) and spatially separates the QD and quencher. This decreases the FRET efficiency and results in enhanced emission from the QD donor.[15] However, the singular response of a turn-on sensor may be difficult to quantify within a complex environment such as a cell. To resolve this issue, Medintz et al. used a luminescent dye in place of the quencher to impart a dual-emissive (i.e. ratiometric) response to DNA.[16] In this design, the ratio of the emission intensities is a calibratable signal that reports the analyte concentration. Moving beyond the molecular beacon approach, Zhang et al. reported a ratiometric emissive QD-based sensor for ssDNA although they used a somewhat complex "sandwich" capture strategy to demonstrate analyte-dependent FRET between a QD donor and ssDNA-dye labelled acceptor.[17] This architecture can also be used in reverse in a displacement strategy where titration of the analyte negates FRET efficiency.[18] There are in fact a very large number of mechanisms of ssDNA sensing using QD FRET donors as recently reviewed by Hildebrandt et al.[19] It is also interesting to note that ssDNA-QD conjugates may also be used as reporters for analytes other than oligonucleotides, such as proteins,[20, 21] illegal drugs,[22] or pH.[23]

Our research into DNA sensing was initially target-oriented rather than focused on method development. As a result, we first examined the use of the most simple and cost effective analytical method of hybridizing water-soluble ssDNA-QD conjugates with the complementary oligonucleotide (the analyte) and staining the resulting dsDNA with a reporter dye. These studies were performed with commercially available materials, specifically 40% octylamine-modified poly(acrylic acid)-encapsulated water-soluble CdSe/ZnS QDs[24] that are commonly used for biological sensing. However, we encountered great difficulty coupling them to amine-functional ssDNA (>10 nucleotides) despite the use of highly efficient methods.[25, 26] As a result, a cap-exchange[27, 28] process was used to create aqueous QDs that can be functionalized with ssDNA with high yields. DNA stains were investigated to evaluate their ability to simultaneously bind to dsDNA and act as a fluorescent FRET acceptor. It was found that PicoGreen functioned acceptably in this regard, although it requires blue-emissive CdZnS/ZnS QD FRET donors. The sum of these developments allowed for the demonstration of a simple, homogeneous ratiometric fluorescence-based analytical method for the quantification of DNA. Control samples demonstrated negligible response from exposure to one basepair-mismatched ssDNA.

EXPERIMENTAL

Materials. Ethidium bromide (EtBr) was purchased from Acros. Cadmium oxide brown (CdO, purum p.a.; >99.0%) and triethylamine (puriss p.a.; >99.5%) were purchased at Fluka. Trioctylphosphine (TOP, 97%) was obtained from Strem. Zinc oxide (ZnO, nanopowder), 1-octadecene (90% technical grade), oleic acid (90% technical grade), sulfur (99.98%), and dodecylamine (98%) were purchased from Sigma-Aldrich. Diethyl zinc ($ZnEt_2$, 95%) and hexamethyldisilathiane ($(TMS)_2S$, 95%) were purchased from Sigma-Aldrich and stored at -20°C in a glove box. Solvents such as 1-butanol (99.5%), chloroform (>99.8%), dichloromethane (>99.8%, dried over activated molecular sieves), isopropanol (>99.5%), methanol (99.9%), and *n*-hexane (>98.5%) were also purchased from Sigma-Aldrich. Oleic acid was recrystallized prior to use,[29] which is essential for obtaining high quality materials reproducibly. See ref. 30 for a tutorial on oleic acid recrystallization. DNA samples were purchased from Integrated DNA Technologies. Initially, 10 nucleotide long amine-functionalized ssDNA was employed, although the data reported here are from the use of longer ssDNA samples. Specifically, both amine and methacrylic phosphoramidite (acrydite) functionalized 5'-/(modifier)/GAG CTG CAC GCT GCC GTC-3' were coupled to water-soluble QDs. The model analyte was 5'-GAC GGC AGC GTG CAG CTC-3'. The one basepair-mismatched sequence used was 5'-GAC GGC AGC ATG CAG CTC-3'. The use of analytes with more mismatches produced results identical to the singly mismatched sample. PicoGreen in DMSO solution was purchased from Life Technologies. Float-A-Lyzer G2 100 KDa MWCO dialysis tubes were purchased from Spectrum Labs.

Characterization. CdZnS/ZnS quantum dots were characterized with a JEOL JEM-3010 operating at 300 kV. UV/Vis absorption spectroscopy was performed with a Varian Cary 300 Bio while fluorescent spectra were measured using a custom-made Fluorolog from HORIBA JobinYvon. Elemental analysis was performed using a Perkin-Elmer flame atomic absorption spectrometer.

Quantum Dot Synthesis. CdSe/CdZnS quantum dots were prepared according to the supporting information of ref. 31. CdZnS/ZnS core-shell quantum dots ~6 nm in diameter were synthesized via an adaptation of refs. 32 and 33. A 100 mL three neck round bottom flask containing 36 mg of CdO, 45 mg of ZnO, 5 g of 1-octadecene, and 1 g of purified oleic acid was heated to 120 °C using a Glas-Col heating mantel and then degassed under vacuum for several hours. During this time, 25 mg of sulfur was dissolved in 1 g of dodecylamine and subsequently degassed under vacuum. At elevated temperatures (>280 °C) the octadecene solution turned from a maroon to a cloudy white color. Near the injection temperature of 310 °C, the solution turned clear and colorless upon which time the sulfur solution was quickly injected into the solvent. The QDs were then grown at 300 °C for 30 minutes to create the CdZnS cores. The CdZnS cores were precipitated with isopropanol and centrifuged to isolate the QDs from the supernatant. After discarding the supernatant, the cores were redispersed into hexane and transferred into a four neck round bottom flask with an attached addition funnel and temperature probe. Next, 4 g of dodecylamine and 5 mL of TOP were added to the flask which was subsequently degassed under vacuum at 80 °C to remove the hexane. The solution was stirred under nitrogen for 1 hour at 120 °C which results in significant brightening of the dots. After the hour, the temperature was increased to 170 °C for ZnS shell growth. Approximately 160 mg of $(TMS)_2S$ and 80 mg of $ZnEt_2$ were added to 7 mL of TOP inside of a glove box. This solution was slowly dripped into the round bottom flask over the course of 20 minutes using an addition funnel. Afterward the solution was left to stir for one hour at a constant temperature of 170 °C. The core-shell quantum were then transferred from the round bottom using 1-butanol into a glass vial and were stored at room temperature. Shown in Fig. 1 are selected characterization results. The spherical QDs are 6.38 ± 0.13 nm in diameter and highly crystalline as shown in TEM microscopy; see Fig. S1 of the supporting information for additional data. Atomic absorption spectroscopy was used to determine the elemental levels (Cd and Zn) in a measured amount

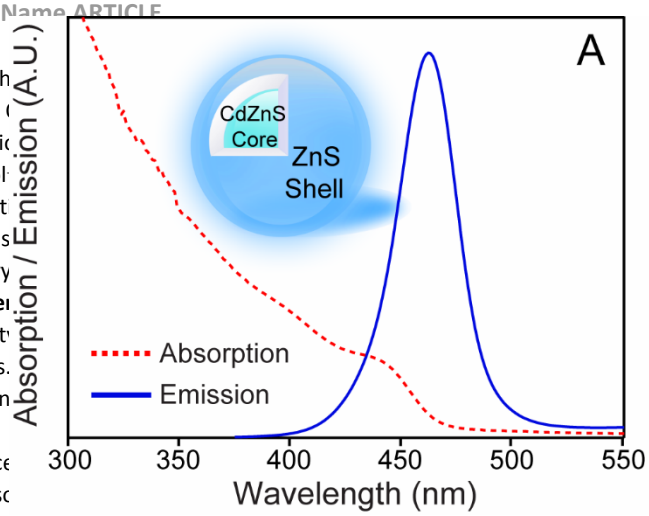

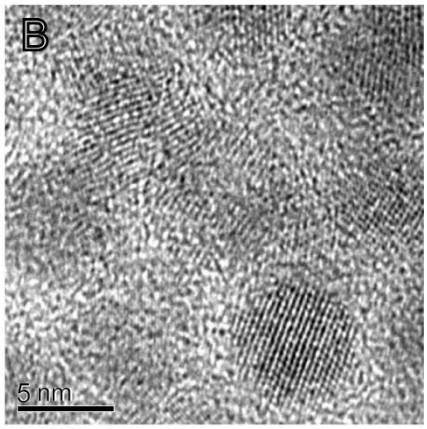

of growth
that the
informati
10^5 L mol
best relat
and pleas
with recry

Wate
40% oct
protocols.
thin silan
reported
reproduce
growth sc

glass vial that was then centrifuged. Next, the supernatant was removed, and the dots were washed with methanol and centrifuged once again. The supernatant was removed, and the QDs were dried in a glass vial under ambient conditions. Next, 5 mL of dry dichloromethane was added to redissolve the QDs. Afterward, 75 μL of 3-mercaptopropyl trimethoxysilane, 8 mg of zinc chloride, and 83 mg of cesium carbonate were added, and the mixture was stirred for 24 hours. Next, the QDs were centrifuged, and the dot-laden supernatant was transferred into a new vial where the nanocrystals were precipitated with hexane and centrifuged again. The supernatant was disposed, and the QDs were dried under ambient conditions. At this point, the QDs can be

Fig. 1 (A) Absorption and emission of a typical CdZnS/ZnS QD sample. (B) TEM micrograph showcases the shape and crystallinity of CdZnS/ZnS nanocrystals.

rendered into water with the addition of ~5 mL of a 0.1 M NaOH solution, although some samples needed to be stirred overnight to achieve a high phase transfer yield. The samples were purified to neutrality by overnight dialysis with a Float-A-Lyzer tube to remove excess ligands and base.

ssDNA-QD Conjugation. Amide bond formation. Polymer-encapsulated CdSe/CdZnS QDs were conjugated to 10 nucleotide long amine-functional ssDNA using poly(ethylene glycol) carbodiimide[25] and similar reagents.[26] Samples were prepared according to the protocols in these references, and were purified with dialysis and characterized optically; see Fig. S2 of the SI. These samples were used as FRET sensors for ssDNA detection using the strategy outlined in Fig. S3, the data from which are presented in Fig. S4. However, this protocol failed to produce ssDNA-QD conjugates with longer amine-functional oligonucleotides (>10), which places obvious limits on the selectivity of such a sensor system. As such, we developed another methodology to couple larger oligomers to QDs, although we had to abandon the use of encapsulated dots.

Michael Addition. A second coupling methodology was developed for cap exchanged dots. For these samples, ~220 nmol of single-stranded acrydite-modified oligonucleotide was added to 10 mL of a 4.6 × 10^{-7} M solution of thiol-functional silane cap-exchanged water-solubilized CdZnS/ZnS QDs along with sub-milligram quantities of sodium chloride. The sample was stirred for 24 hours and then dialyzed overnight using a dialysis tube. The conjugation efficiency was estimated from absorption spectroscopy by subtracting the ssDNA-QD spectrum from a blank QD; see Fig. S5 of the SI. The excess absorption at 260 nm must result from QD-bound ssDNA, and the amount of ssDNA was determined using the manufacturer's quoted optical density at this wavelength. For the sample presented in this manuscript, an 80% conjugation efficiency was determined, resulting in an ssDNA:QD ratio of 39:1.

Titration with DNA-intercalating dyes. Ethidium bromide. First, dsDNA-CdSe/ZnS dot conjugates were prepared by incubating an excess of complementary oligonucleotides to ssDNA-QDs followed by dialysis. Successful hybridization was confirmed with UV/Vis absorption spectroscopy. Next, blank water-soluble CdSe/ZnS QDs, ssDNA-CdSe/ZnS, and dsDNA-CdSe conjugates (~3.4×10^{-7} M) were exposed to increasing levels of ethidium bromide and characterized using fluorescence spectroscopy. The results from these experiments are shown in Fig. S4 and are summarized in Fig. 2. As discussed below, results from ethidium bromide staining of dsDNA-QDs and control samples revealed that this method is not suitable for DNA sensing. Further studies and control experiments were not examined in favor of developing a more productive method.

PicoGreen. An alternative method was employed using DNA-CdZnS/ZnS conjugates exposed to the intercalating dye PicoGreen. Blank dots and ssDNA-QD sensors were divided into several 1 mL samples. The blank cap-exchanged QD sample was not functionalized with ssDNA nor was exposed to DNA analytes. Three ssDNA-QD conjugates were incubated with 100%, 50%, and 10% equivalences of the complementary ssDNA analyte as determined from the total quantity of ssDNA in the conjugates. Three more ssDNA-QD samples were exposed to 100%, 50%, and 10% equivalences of a one basepair-mismatched ssDNA analyte, again relative to the total quantity of ssDNA in the quantum dot conjugate. Additional sub-milligram quantities of sodium chloride were added to all samples, which were then incubated in a warm water bath (50 °C) for 1 hour and then overnight at room temperature while slowly stirring. UV/Vis spectroscopy was used to characterize the samples, see for example Fig. S5. All samples were titrated with PicoGreen while monitoring the fluorescence response using a Fluoromax spectrofluorimeter. Samples were excited at 360 nm and the emission was measured from 375 nm to 650 nm. The excitation and emission slits were set to 1 nm and the integration time was set to 1 second. The excitation wavelength was chosen to be far from the first absorption feature of the dye to maximize excitation of the quantum dots.

We attempted to create an assay where a solution consisting of a mixture of ssDNA-QD and PicoGreen was titrated with the complementary oligonucleotide analyte. This method failed to produce an optical response, which leads us to believe that PicoGreen coordinates to ssDNA and prevents hybridization, albeit in a non-fluorescent state.

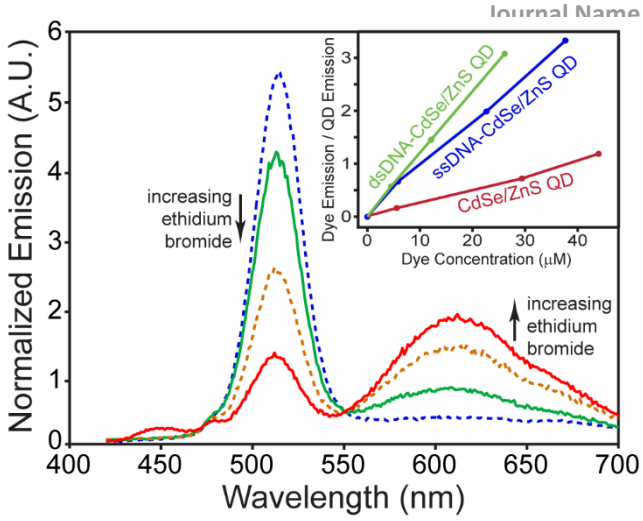

RESULTS AND DISCUSSION

Sensing with dsDNA-CdSe/ZnS QDs and ethidium bromide. Our initial studies focused on the detection of a particular DNA sequence rather than the development of an analytical method. As such, we initially examined a previously reported procedure for unlabeled ssDNA sensing using CdSe/ZnS quantum dots.[36, 37] Some alterations were made to enhance technological transferability, such as the use of water-soluble polymer-encapsulated dots[24] rather than cap-exchanged QDs as most commercially available nanocrystal materials are coated with polymers. They were chemically conjugated to short amine-modified oligonucleotides according to previously published protocols.[25, 26] After removal of unreacted oligos and reagents with dialysis, the absorption spectra of the dots before and after conjugation revealed obvious DNA characteristics, see Fig. S2 of the supporting information. Longer oligonucleotides could not be conjugated to QDs, which we attribute to electrostatic repulsion. After exposing the ssDNA-QD to the compliment to form dsDNA-QD as confirmed by UV/Vis spectroscopy, ethidium bromide was titrated into these samples as well as blank QD and ssDNA-QD controls. Shown in Fig. 2 are the normalized emission spectra of dsDNA-QD as a function of increasing EtBr exposure. As seen in ref. 37, emission from the QDs is quenched due to energy transfer to the emissive dye. The responses of this sample and the controls were quantified by dividing the integrated dye emission by the same of the quantum dot as shown in the inset of Fig. 2. Unfortunately, the control ssDNA-QD had a near-identical responses. This is somewhat perplexing as ethidium bromide has been used to differentiate between ssDNA and dsDNA,[38] yet other groups have shown that EtBr has an identical response to both ssDNA and dsDNA[39, 40] as observed here. These seemingly contradictory observations have been attributed to the strong dependence of ethidium bromide fluorescence on the EtBr to DNA ratio[41] that may cause the dye to appear somewhat falsely selective for dsDNA at high EtBr loading levels.[38] Given the difficulties in the synthesis of QD-DNA conjugates and the fact that the use of EtBr is problematic, an alternative method to quantify DNA was developed.

Fig. 2 The normalized (by total area) emission spectra of a CdSe/CdZnS quantum dot conjugated to dsDNA in the presence of increasing levels of the DNA intercalating dye ethidium bromide. Inset: ratio of integrated dye to QD emission as EtBr is added. The data show that the response of both dsDNA-QD and the control ssDNA-QD are almost identical, negating the use of this method as a strategy to sense ssDNA analytes.

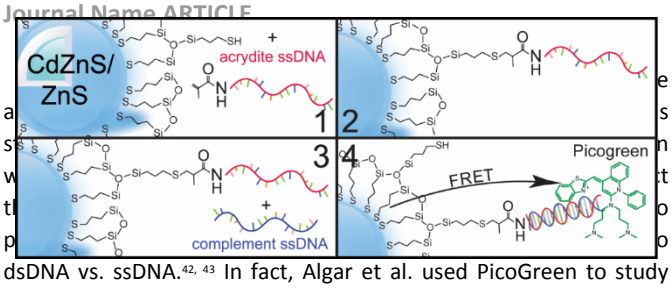

Fig. 3 The strategy to synthesize a cap-exchanged ssDNA-CdZnS/ZnS QD-FRET ssDNA sensor. (1,2) Conjugation of the QD to an acrydite modified oligonucleotide. (3) dsDNA is formed in the presence of the complementary ssDNA analyte. (4) Upon addition of dsDNA intercalating PicoGreen dye, FRET from the QD to the dye is observed as shown in Fig. 4.

polymer-encapsulation method with 40% octylamine-modified polyacrylic acid[24] was as efficient for these dots as for CdSe/CdZnS nanocrystals. Unfortunately, the same difficulties were encountered with conjugating long (> 10 nucleotides) amine-functional ssDNA to CdZnS/ZnS QDs as were observed with CdSe/ZnS nanocrystals. In fact, the situation was worse as it was found that even simple exposure to oligos longer than 10 nucleotides often caused the polymer-encapsulated CdZnS/ZnS QDs to precipitate. Even when precipitation could be mitigated, the conjugation efficiencies were very low.

Given these issues, a new strategy was adopted as outlined in Fig. 3. Specifically, the QDs were first water-solubilized via cap-exchange with a monolayer of organic silane.[28] This method renders significantly more compact QDs compared to encapsulated dots, and the water-soluble dispersion is stable for months under bench top conditions. Most importantly, the outer layer contains free thiols that can react with methacrylic phosphoramidite (aka "acrydite") functional ssDNA,[45] yet do not cross-link among dsDNA vs. ssDNA.[42, 43] In fact, Algar et al. used PicoGreen to study the hybridization of DNA on QD conjugates;[36] however, the group did not use the dye in a ratiometric detection scheme likely due to the fact that PicoGreen's absorption is below 500 nm, making it incompatible with green-emissive CdSe/CdZnS QDs as FRET donors. As a result, we developed a procedure based on recent publications[32, 33] to create bright blue-emissive CdZnS/ZnS QDs for use with PicoGreen for the quantification of dsDNA.

There are two noteworthy aspects concerning the synthesis of these nanocrystals. First, it is necessary to use zinc in the core synthesis, otherwise the materials only display deep trap emission. Also, the precursors include cadmium and zinc oleate prepared from their respective metal oxides. As cadmium oxide reacts with the oleic acid first, we believe that the corresponding cadmium oleate is more reactive than the zinc analog towards sulfur. As such, the cadmium reacts first upon injection of sulfur to create a CdS-rich interior, and subsequent growth produces a more ZnS-rich outer layer. Unfortunately, this is difficult to prove without extensive TEM analysis, although the fact that surface state emission is suppressed supports this model.[44] The second issue to note during the synthesis of the cores is that the purity of oleic acid matters. Use of highly purified oleic acid can assure the relative absence of deep-trap emission. Upon overcoating, the fluorescence was enhanced, resulting in a best result of 80% quantum yield relative to Coumarin 102 dye.

Water solubilization and ssDNA conjugation. The blue emission of CdZnS/ZnS QDs should make them good FRET donors to PicoGreen acceptors, but they must be water-solubilized and conjugated to ssDNA first. It was found that the

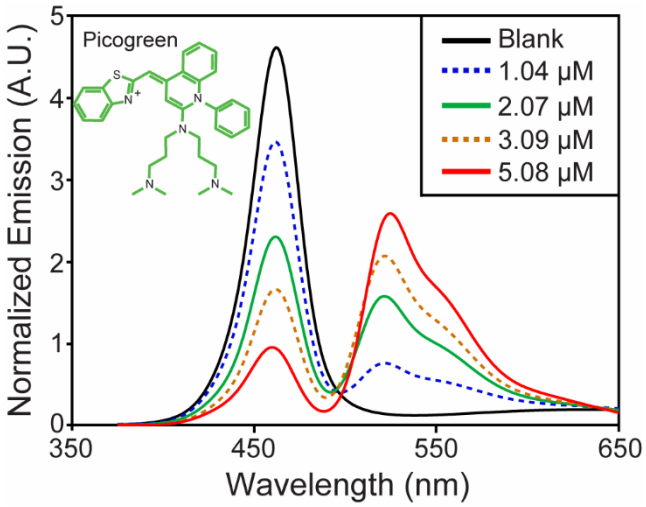

Fig. 4 The normalized (by total area) emission spectra from an aqueous ssDNA-QD conjugate hybridized with a 100% equivalence of the ssDNA's compliment as a function of the addition of PicoGreen dsDNA intercalating dye (concentrations shown in inset).

themselves most likely due to electrostatic repulsion. The ssDNA-QD conjugate was prepared by simply mixing the two followed by purification using dialysis, which is a significant advancement compared to other multistep protocols for synthesizing the same. Conjugation with longer oligos did not appear to be an issue as well. This protocol was determined to have an 80% coupling efficiency resulting in a 39:1 ssDNA to dot conjugate ratio. Analysis of the optical properties of the resultant materials as shown in Fig. S6 indicate that the dots can make good FRET donors to PicoGreen with a FRET characteristic lengthscale (R_0) of 3.6 nm; see the supporting information for additional FRET characterization.

Titration with PicoGreen. Having resolved several issues with the synthesis of the appropriate color QDs and ssDNA conjugation chemistry, we then began to study the sensing of unlabeled complementary ssDNA as well as control samples. Our initial protocol involved titrating an equivalent of the complementary ssDNA analyte into a mixture of ssDNA-QD and PicoGreen dye. It was hypothesized that dsDNA would first form and that PicoGreen would next intercalate into it, resulting in a quantifiable increase in FRET from the QD to PicoGreen as a function of DNA analyte titration. However, there was no optical response to the addition of the complementary ssDNA over any reasonable period of time. We believe that this may have been due to the dye binding to the probes' ssDNA, in a non-fluorescent state, in such a way that it prevented hybridization. In support of this is the fact that a very strong ratiometric fluorescent response is observed when the assay is run in reverse by incubating the sensor with the analyte first and then titrating in the dye.

These results led to the development of a protocol where ssDNA-QD were first incubated with the complement or a one basepair-mismatched ssDNA control. This was performed using either a 100%, 50%, or 10% equivalence of analyte compared to the oligonucleotide content of the ssDNA-QD sensors. Next, the emission spectra were measured as the PicoGreen dsDNA intercalating dye solution was added in increasing portions. The results for the addition of the complementary ssDNA at 100% equivalency are shown in Fig. 4. There is a significant level of QD quenching that is accompanied by increasing PicoGreen emission upon titration. The same ssDNA modified QDs were exposed to 50%

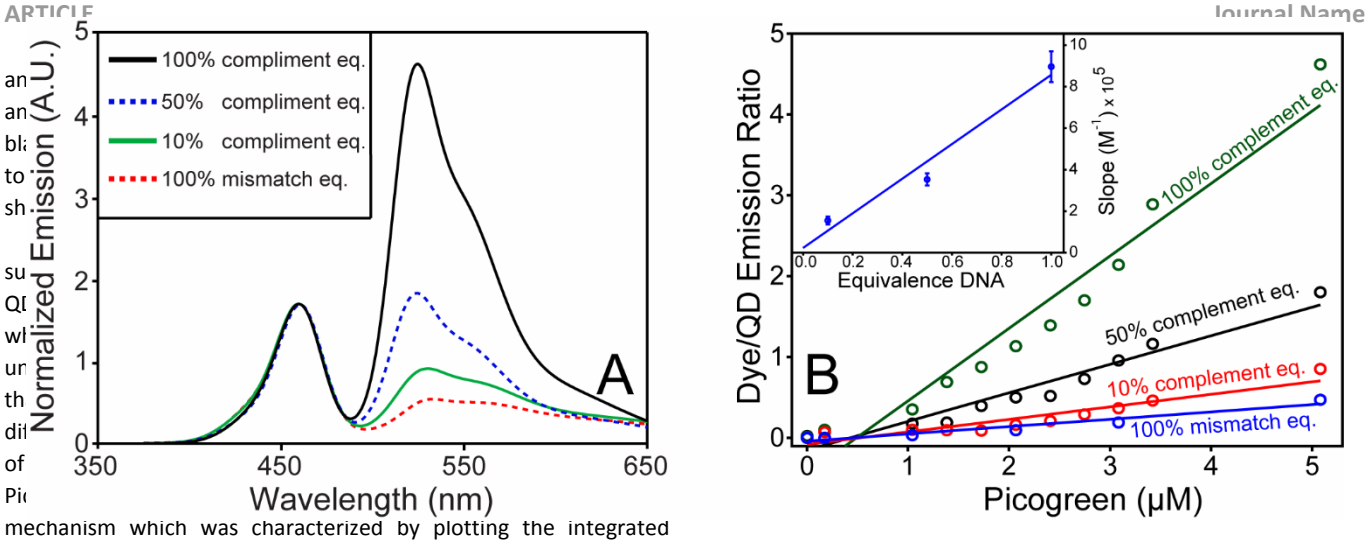

mechanism which was characterized by plotting the integrated dye/QD emission ratio vs. the dye concentration as a function of dsDNA loading as shown in Fig. 5B. We will first examine the photophysical properties of the various DNA + QD + dye systems, and follow by a discussion on the protocol for QD-based ratiometric sensing of unlabeled DNA may perform with this platform.

Mechanism. A natural question is to determine whether the mechanism of Fig. 3 (panel 4) is functioning, rather than collisional quenching of the QD donor due to non-specifically bound dye. To this end a Stern-Volmer analyses of the dye-

Fig. 5 (A) Emission spectra of ssDNA-CdZnS/ZnS QD conjugates stained with 5.08 μM of PicoGreen solution as a function of complementary ssDNA analyte exposure. The data are normalized to the quantum dot emission. (B) The integrated dye emission divided by the same of the QD as a function of increasing exposure to PicoGreen. Inset: The slope of the response is a function of the equivalence of analyte exposure relative to the QD-bound ssDNA recognition element.

induced quenching of the donor was performed for all the samples discussed herein; these data are shown in Fig. S8 and summarized in Table S1 of the supporting information. It was found that the dye quenches the fluorescence of both the blank QDs and ssDNA-QDs that were incubated with 100% equivalent of a one basepair-mismatched analytes. Specifically, a plot of I_0/I vs. dye concentration generates a straight line with a large (~10^5 M^{-1}) K_{sv} for both control samples. Such a high Stern-Volmer equilibrium constant cannot result from collisional quenching of the QDs,[46] which suggests rather sensibly that the cationic PicoGreen dye coordinates to the surface of the negatively charged QDs regardless of whether or not the sample has been functionalized with ssDNA. The data are significantly different for ssDNA-QDs that have been exposed to increasing quantities of the complementary analyte to form dsDNA-QD conjugates. The I_0/I vs. dye concentration data display two response regimes. A minor component was observed with a very high K_{sv} over a PicoGreen concentration that corresponds to a dye to QD ratio of ~1. This response then saturates, and is followed by a second dynamic with a K_{sv} that is lower than that observed in the control samples yet is still far too high to be due to non-specific collisional quenching. Due to the concomitant increase in dye emission that is consistently observed with increasing PicoGreen concentration as shown in Fig. 5A, we propose that the dye is intercalating to dsDNA.

To summarize, PicoGreen is a cationic dye that coordinates to the surface of anionic silane-coated CdZnS/ZnS QDs and quenches its emission. This occurs regardless of whether the dots have been functionalized with ssDNA. However, the dye intercalates into dsDNA if it is present to serve a dual role of QD quencher and emissive reporter. This is why Stern-Volmer analyses of the various dsDNA-QD-dye systems demonstrate two quenching components, both of which have very high association constants. Titrating the dsDNA-QD conjugates with PicoGreen beyond a 1:1 ratio results in an enhanced ratiometric response, although the dye no longer quenches the QD fluorescence as efficiently. This is likely due to the fact that increasing the donor:acceptor ratio does not increase the FRET efficiency in a linear manner, and possibly the heterogeneity in the position of the DNA-intercalated dye relative to the QD.

A practical assay. The fact that the sensing motif reported here does not respond to the direct titration of the analyte (complementary ssDNA), but rather a secondary reporter (PicoGreen), engenders the question of how the QD sensor system reported here can realistically function. To this end we first note that the slope of the response of the sensor to dye titration is dependent on the quantity of the analyte. As such, the slope of this response can act as the analytical metric for ssDNA quantification. Specifically, one can take an ssDNA-QD conjugate, incubate it with an unknown, and then titrate the solution with PicoGreen dye to determine the slope of the fluorescence ratiometric response. The concentration of the dye titrant would simply need to be above the kD with DNA, which is ~45 nM in buffer.[47] The response can be used to determine the amount of complementary analyte present as a percentage of the known quantity of oligos in the ssDNA-QD sensor solution, so long as the equivalency is above the limit of detection

(LOD). To determine the LOD, if we factor the slope of the response to exposure to one basepair-mismatched ssDNA (at 100% equivalence) into the regression of the response vs. complementary ssDNA analyte equivalence (the line in Fig. 5B inset), the result is that exposure to a single mismatch sequence is the same as exposure to 8.1% equivalence of the complementary sequence. Under the conditions employed here and including a full error analysis discussed in the supporting information, this corresponds to a detection limit of 3.8 nmol of ssDNA.‡ Also note that the detection limit of a ratiometric sensor can be scaled proportionally with sensor concentration so long as the emission signal integrity is not seriously compromised.

Conclusions

In summary, we have developed on a mechanism for ratiometric fluorescent QD-based unlabeled ssDNA sensing where a dsDNA-QD complex is stained with an energy-accepting dye. It was found that PicoGreen is essential towards discriminating between the QD-bound ssDNA recognition element vs. the dsDNA that forms due to exposure to the complementary analyte. The use of this dye required the development of blue-emitting CdZnS/ZnS QDs that function as good energy transfer donors to DNA intercalating PicoGreen dye acceptors. Furthermore, polymer-encapsulated QDs were found to be problematic when conjugating ssDNA that are greater than 10 nucleotides in length, likely due to electrostatic interactions. The use of dots that were cap-exchanged with a thiol-functional silane to impart water-solubility resolved this issue. The surface-bound thiol groups allowed for the conjugation of acrydite-functional ssDNA in a single high-yielding reagentless step. An assay was developed where the sensor is first preincubated with the analyte and then titrated with the DNA intercalating dye. The response is a quantifiable function of the quantity of analyte, and the system has a minimal response to control samples. As this is a ratiometric measurement, the absolute detection limit is scalable with the sensor quantity and is only balanced with the need to retain a reasonable signal to noise ratio for analyte quantification.

Acknowledgements

This work was supported by the University of Illinois at Chicago and the UIC Chancellor's Discovery Fund as well as the U.S. Air Force Surgeon General's Office of Modernization under Contract FA7014-07-C-0047. Acknowledgment is made to the Donors of the American Chemical Society Petroleum Research Fund for partial support of this research. We would like to thank Jonathan Halpert for helpful discussions on CdZnS/ZnS quantum dot synthesis and Tim Keiderling for providing some ssDNA samples.

Notes and references

‡ This figure takes into account the upper limit of the standard deviation of the calculated limit of detection. See the supporting information for the full details.

1. C. Bettegowda, M. Sausen, R. J. Leary, I. Kinde, Y. X. Wang, N. Agrawal, B. R. Bartlett, H. Wang, B. Luber, R. M. Alani, E. S. Antonarakis, N. S. Azad, A. Bardelli, H. Brem, J. L. Cameron, C. C. Lee, L. A. Fecher, G. L. Gallia, P. Gibbs, D. Le, R. L. Giuntoli, M. Goggins, M. D. Hogarty, M. Holdhoff, S. M. Hong, Y. C. Jiao, H. H. Juhl, J. J. Kim, G. Siravegna, D. A. Laheru, C. Lauricella, M. Lim, E. J. Lipson, S. K. N. Marie, G. J. Netto, K. S. Oliner, A. Olivi, L. Olsson, G. J. Riggins, A. Sartore-Bianchi, K. Schmidt, I. M. Shih, S. M. Oba-Shinjo, S. Siena, D. Theodorescu, J. N. Tie, T. T. Harkins, S. Veronese, T. L. Wang, J. D. Weingart, C. L. Wolfgang, L. D. Wood, D. M. Xing, R. H. Hruban, J. Wu, P. J. Allen, C. M. Schmidt, M. A. Choti, V. E. Velculescu, K. W. Kinzler, B. Vogelstein, N. Papadopoulos and A. J. Luis, *Sci. Transl. Med.*, 2014, **6**, 224ra24.
2. J. H. Mermin, M. Holodniy, D. A. Katzenstein and T. C. Merigan, *J. Infect. Dis.*, 1991, **164**, 769-772.
3. H. Shirai, M. Nishibuchi, T. Ramamurthy, S. K. Bhattacharya, S. C. Pal and Y. Takeda, *J. Clin. Microbiol.*, 1991, **29**, 2517-2521.
4. S. H. Lee, V. S. Vigliotti, J. S. Vigliotti, W. Jones and S. Pappu, *Am. J. Clin. Pathol.*, 2010, **133**, 569-576.
5. R. C. Somers, M. G. Bawendi and D. G. Nocera, *Chem. Soc. Rev.*, 2007, **36**, 579-591.
6. X. Michalet, F. F. Pinaud, L. A. Bentolila, J. M. Tsay, S. Doose, J. J. Li, G. Sundaresan, A. M. Wu, S. S. Gambhir and S. Weiss, *Science*, 2005, **307**, 538-544.
7. K. M. Fichter, M. Flajolet, P. Greengard and T. Q. Vu, *Proc. Natl. Acad. Sci. U. S. A.*, 2010, **107**, 18658-18663.
8. C. M. Tyrakowski and P. T. Snee, *Phys. Chem. Chem. Phys.*, 2014, **16**, 837-855.
9. Y. Kim, D. Sohn and W. H. Tan, *Int. J. Clin. Exp. Pathol.*, 2008, **1**, 105-116.
10. J. H. Kim, D. Morikis and M. Ozkan, *Sensor. Actuat. B-Chem.*, 2004, **102**, 315-319.
11. N. C. Cady, A. D. Strickland and C. A. Batt, *Mol. Cell. Probes*, 2007, **21**, 116-124.
12. D. M. Willard, L. L. Carillo, J. Jung and A. Van Orden, *Nano Lett.*, 2001, **1**, 469-474.
13. I. L. Medintz, A. R. Clapp, H. Mattoussi, E. R. Goldman, B. Fisher and J. M. Mauro, *Nat. Mater.*, 2003, **2**, 630-638.
14. T. Pons, I. L. Medintz, K. E. Sapsford, S. Higashiya, A. F. Grimes, D. S. English and H. Mattoussi, *Nano Lett.*, 2007, **7**, 3157-3164.
15. S. Tyagi and F. R. Kramer, *Nat. Biotechnol.*, 1996, **14**, 303-308.
16. I. L. Medintz, L. Berti, T. Pons, A. F. Grimes, D. S. English, A. Alessandrini, P. Facci and H. Mattoussi, *Nano Lett.*, 2007, **7**, 1741-1748.
17. C. Y. Zhang, H. C. Yeh, M. T. Kuroki and T. H. Wang, *Nat. Mater.*, 2005, **4**, 826-831.
18. C. H. Vannoy, L. Chong, C. Le and U. J. Krull, *Anal. Chim. Acta*, 2013, **759**, 92-99.
19. N. Hildebrandt, C. M. Spillmann, W. R. Algar, T. Pons, M. H. Stewart, E. Oh, K. Susumu, S. A. Díaz, J. B. Delehanty and I. L. Medintz, *Chem. Rev. (Washington, DC, U. S.)*, 2016, **asap**.
20. M. Levy, S. F. Cater and A. D. Ellington, *ChemBioChem*, 2005, **6**, 2163-2166.
21. C. M. Tyrakowski and P. T. Snee, *Anal. Chem.*, 2014, **86**, 2380-2386.
22. C. Y. Zhang and L. W. Johnson, *Anal. Chem.*, 2009, **81**, 3051-3055.
23. E. R. Kay, J. Lee, D. G. Nocera and M. G. Bawendi, *Angew. Chem., Int. Ed.*, 2013, **52**, 1165-1169.
24. X. Y. Wu, H. J. Liu, J. Q. Liu, K. N. Haley, J. A. Treadway, J. P. Larson, N. F. Ge, F. Peale and M. P. Bruchez, *Nat. Biotechnol.*, 2003, **21**, 41-46.
25. H. Y. Shen, A. M. Jawaid and P. T. Snee, *ACS Nano*, 2009, **3**, 915-923.
26. X. Zhang, S. Mohandessi, L. W. Miller and P. T. Snee, *Chem. Commun. (Cambridge, U. K.)*, 2011, **47**, 3532–3534.
27. D. Liu and P. T. Snee, *ACS Nano*, 2011, **5**, 546-550.

28. X. Zhang, A. Shamirian, A. M. Jawaid, C. M. Tyrakowski, L. E. Page, A. Das, O. Chen, A. Isovic, A. Hassan and P. T. Snee, *Small*, 2015, **11**, 6091-6096.
29. R. L. Arudi, M. W. Sutherland and B. H. J. Bielski, *J. Lipid Res.*, 1983, **24**, 485-488.
30. https://www.youtube.com/watch?v=1Uh2MCR1eRs.
31. P. T. Snee, C. M. Tyrakowski, A. Isovic, L. E. Page and A. M. Jawaid, *J. Phys. Chem. C*, 2011, **115**, 19578-19582.
32. X. H. Zhong, Y. Y. Feng, W. Knoll and M. Y. Han, *J. Am. Chem. Soc.*, 2003, **125**, 13559-13563.
33. J. S. Steckel, J. P. Zimmer, S. Coe-Sullivan, N. E. Stott, V. Bulovic and M. G. Bawendi, *Angew. Chem., Int. Ed.*, 2004, **43**, 2154-2158.
34. W. W. Yu, L. H. Qu, W. Z. Guo and X. G. Peng, *Chem. Mater.*, 2003, **15**, 2854-2860.
35. Y. Chen, R. Thakar and P. T. Snee, *J. Am. Chem. Soc.*, 2008, **130**, 3744-3745.
36. W. R. Algar and U. J. Krull, *Anal. Chim. Acta*, 2007, **581**, 193-201.
37. D. J. Zhou, L. M. Ying, X. Hong, E. A. Hall, C. Abell and D. Klenerman, *Langmuir*, 2008, **24**, 1659-1664.
38. H. C. Birnboim and J. J. Jevcak, *Cancer Res.*, 1981, **41**, 1889-1892.
39. L. Beach, C. Schweitzer and J. C. Scaiano, *Org. Biomol. Chem.*, 2003, **1**, 450-451.
40. G. Cosa, K. S. Focsaneanu, J. R. N. McLean, J. P. McNamee and J. C. Scaiano, *Photochem. Photobiol.*, 2001, **73**, 585-599.
41. M. D. Dutton, R. J. Varhol and D. G. Dixon, *Anal. Biochem.*, 1995, **230**, 353-355.
42. V. L. Singer, L. J. Jones, S. T. Yue and R. P. Haugland, *Anal. Biochem.*, 1997, **249**, 228-238.
43. S. J. Ahn, J. Costa and J. R. Emanuel, *Nucleic Acids Res.*, 1996, **24**, 2623-2625.
44. J. McBride, J. Treadway, L. C. Feldman, S. J. Pennycook and S. J. Rosenthal, *Nano Lett.*, 2006, **6**, 1496-1501.
45. D. P. Nair, M. Podgorski, S. Chatani, T. Gong, W. X. Xi, C. R. Fenoli and C. N. Bowman, *Chem. Mater.*, 2014, **26**, 724-744.
46. S. Sadhu and A. Patra, *Appl. Phys. Lett.*, 2008, **93**, 183104.
47. A. I. Dragan, J. R. Casas-Finet, E. S. Bishop, R. J. Strouse, M. A. Schenerman and C. D. Geddes, *Biophys. J.,* 2010, **99**, 3010–3019.